



An efficient solution of system of generalized Abel integral equations using Bernstein polynomials wavelet bases

Shweta Pandey¹ · Sandeep Dixit² · S. R. Verma¹

Received: 13 January 2020 / Accepted: 30 June 2020 / Published online: 14 July 2020
© Islamic Azad University 2020

Abstract

This work introduces a direct method based on orthonormal Bernstein polynomials wavelet bases, to present a stable algorithm for numerical inversion of a system of generalized Abel integral equations. The application of all the currently existing numerical inversion methods was strictly limited to only one portion of the generalized Abel integral equations. The proposed method is quite accurate, and several numerical illustrations demonstrate the convergence and utilization of the proposed method compared to some of the preexisting numerical solution techniques. The permanence of the numerical result under the effect of small perturbation in input data has been examined, which is depicted with the use of numerical illustrations.

Keywords Bernstein polynomials · Abel inversion · Wavelet bases · System of generalized Abel integral equations

Mathematics Subject Classification 65T60 · 45F15 · 65M12

Introduction

In this paper, we propose the method of an approximate numerical inversion for the system of generalized Abel integral equations given by

$$\left. \begin{aligned} \rho_1(s) \int_a^s \frac{u^{\beta-1} \varepsilon_1(u) du}{(s^\beta - u^\beta)^\alpha} + \rho_2(s) \int_s^b \frac{u^{\beta-1} \varepsilon_2(u) du}{(u^\beta - s^\beta)^\alpha} &= I_1(s) \\ \omega_1(s) \int_s^b \frac{u^{\beta-1} \varepsilon_1(u) du}{(u^\beta - s^\beta)^\alpha} + \omega_2(s) \int_a^s \frac{u^{\beta-1} \varepsilon_2(u) du}{(s^\beta - u^\beta)^\alpha} &= I_2(s) \end{aligned} \right\}; s \in (a, b); 0 < \alpha < 1, \beta \geq 1, \quad (1)$$

where the coefficients $\rho_1(s)$, $\rho_2(s)$, $\omega_1(s)$, $\omega_2(s)$ must not vanish simultaneously and $I_1(s)$, $I_2(s)$ are the intensity functions.

The system of generalized Abel integral equations in Eq. (1) holds substantial significance in various spheres. It is considered as a mathematical model in the various fields such as water wave scattering [1], plasma spectroscopy [2],

elasticity [3], mathematical physics, astrophysics, seismology, solid mechanics [4, 5].

There are various numerical methods to find the solution of different kinds of integral equations, such as Maleknejad et al. proposed Legendre wavelets and rationalized

Haar wavelet methods [6, 7], Derili et al. proposed two-dimensional wavelets method [8] and Mandal et al. used the Daubechies scale function [9] method. Several other methods [10–14] have been previously used for the numerical inversion of the system of generalized Abel integral equations. In 1976, Lowengrub [10] showed that certain mixed boundary value problems arising in the classical theory of elasticity converted to the new problem in the form of functions $\varepsilon_1(u)$ and $\varepsilon_2(u)$, these functions satisfy the system in Eq. (1). Lowengrub and Waltson [11] provided a method based on converting the system of generalized Abel integral equations into an equivalent boundary value problem of coupled Riemann–Hilbert type. Some particular generalized system of Abel integral equations solved by creating an equivalent system of singular integral equation in [12].

✉ Sandeep Dixit
SDIXIT@ddn.upes.ac.in

¹ Department of Mathematics and Statistics, Gurukula Kangri Vishwavidyalaya, Haridwar 249404, India

² Department of Mathematics, University of Petroleum and Energy Studies, Dehra Dun 248007, India

Mandal et al. [13] have solved the system with the implementation of fractional calculus. In [14], Mandal and Pandey gave the numerical solution of the system of generalized Abel integral equations through the Bernstein polynomials bases. Jafarian et al. also used the Bernstein polynomial method [15] and Bernstein collocation method [16] for obtaining the solution of the system of integral equations and Abel integral equations, respectively.

This paper aims to give a new and user friendly algorithm for the numerical inversion of the system of generalized Abel integral equation, based on Bernstein polynomials orthonormal wavelet bases. Numerical examples have been provided to illustrate the convergence and stability of the method.

Bernstein polynomials orthonormal wavelet bases

A class of functions, which is obtained by dilation and translation of a single function known as mother wavelet [17]. The continuous variation of the dilation and translation parameters c and d gives the following continuous wavelet bases [18]

$$\psi_{c,d}(u) = |c|^{-1/2} \psi\left(\frac{u-d}{c}\right), \quad c, d \in \mathbb{R}, \quad c \neq 0. \tag{2}$$

If the parameters c and d are regulated to $c = 2^{-k}$; $d = n2^{-k}$, then obtained a family of discrete wavelets from the above equation,

$$\psi_{k,n}(u) = 2^{k/2} \psi(2^k u - n); \quad k, n \in \mathbb{Z}.$$

The Bernstein polynomials characterized over the interval $[0, 1]$ are given as;

$$B_{i,n}(y) = \binom{n}{i} y^i (1-y)^{n-i}; \quad \forall i = 0, 1, 2, \dots, n. \tag{3}$$

Some significant characteristics of Bernstein polynomials are:

- The sum of all Bernstein polynomials of degree n is always one

$$\sum_{i=0}^n B_{i,n}(y) = \sum_{i=0}^n \binom{n}{i} y^i (1-y)^{n-i} = (1-y+y)^n = 1.$$

- $B_{i,n}(y) \geq 0$ for all $y \in [0, 1]$.
- $B_{n-i,n}(1-y) = B_{i,n}(y)$.

The recurrence formula to obtain Bernstein polynomial of degree less than n using Bernstein polynomials of degree n is

$$B_{i,n-1}(y) = \left(\frac{n-i}{n}\right) B_{i,n}(y) + \left(\frac{1+i}{n}\right) B_{i+1,n}(y).$$

The expansion of any polynomial $P(y)$ of degree n can be expressed in terms of a linear combination of $B_{i,n}(y)$

$$P(y) = \sum_{i=0}^n \beta_i B_{i,n}(y), \quad n \geq 1.$$

where β_i is called Bernstein polynomials coefficients, these polynomials are not orthonormal, so we used the Gram–Schmidt process [19] to get orthonormal polynomials, which are denoted by $b_i(y)$ given in “Appendix 1”.

We are taking orthonormal Bernstein polynomials for $N=7$, which are shown graphically in Fig. 1.

The four arguments in the Bernstein polynomials orthonormal wavelet bases $\psi_{m,n}(u) = \psi(k, m, n, u)$, where $m = 0, 1, \dots, 2^k - 1$ and $k = 0, 1, 2, \dots$ are translation and dilation parameters, respectively, $n = 0, 1, \dots, N$ is the order of Bernstein polynomial and the independent variable u is lying in the closed interval $[0, 1]$. The orthonormal wavelet bases $\psi_{m,n}(u)$ are given in [20] on the interval $[0, 1]$, such as

$$\psi_{m,n}(u) = \begin{cases} 2^{k/2} b_n(2^k u - m) & \frac{m}{2^k} \leq u < \frac{m+1}{2^k} \\ 0 & \text{otherwise} \end{cases}, \tag{4}$$

where $2^{k/2}$ is the orthonormality factor, for the dyadic form of orthonormal Bernstein polynomials wavelet bases of the order n we are setting parameters $c = 2^{-k}$ and $d = m2^{-k}$ in Eq. (2).

Now, for $k = 0; N = 7$, there are eight, and for $k = 1; N = 7$, sixteen basis elements of orthonormal wavelet bases are obtained [21].

Function approximation

Let us consider $f \in L^2[0, 1]$, then may be written as the following expansion of $f(u)$ on the closed interval $[0, 1]$

$$f(u) = \sum_{m=0}^{\infty} \sum_{n=0}^{\infty} c_{mn} \psi_{mn}(u), \tag{5}$$

where $\langle \cdot, \cdot \rangle$ is the inner product on the Hilbert space, and $c_{mn} = \langle f(\cdot), \psi_{mn}(\cdot) \rangle$ be the wavelet coefficients. We truncate the infinite series in Eq. (5) at the levels $m = 2^k - 1$ and $n = N$, then obtained an approximate version of these series such as

$$f(u) \approx \sum_{m=0}^{2^k-1} \sum_{n=0}^N c_{mn} \psi_{mn}(u) = C^T \Psi(u), \tag{6}$$

where C and Ψ are $2^k(N+1) \times 1$ order matrices given by

$$C = [c_{00}, \dots, c_{0N}; c_{10}, \dots, c_{1N}; \dots; c_{(2^k-1)0}, \dots, c_{(2^k-1)N}]^T, \tag{7}$$

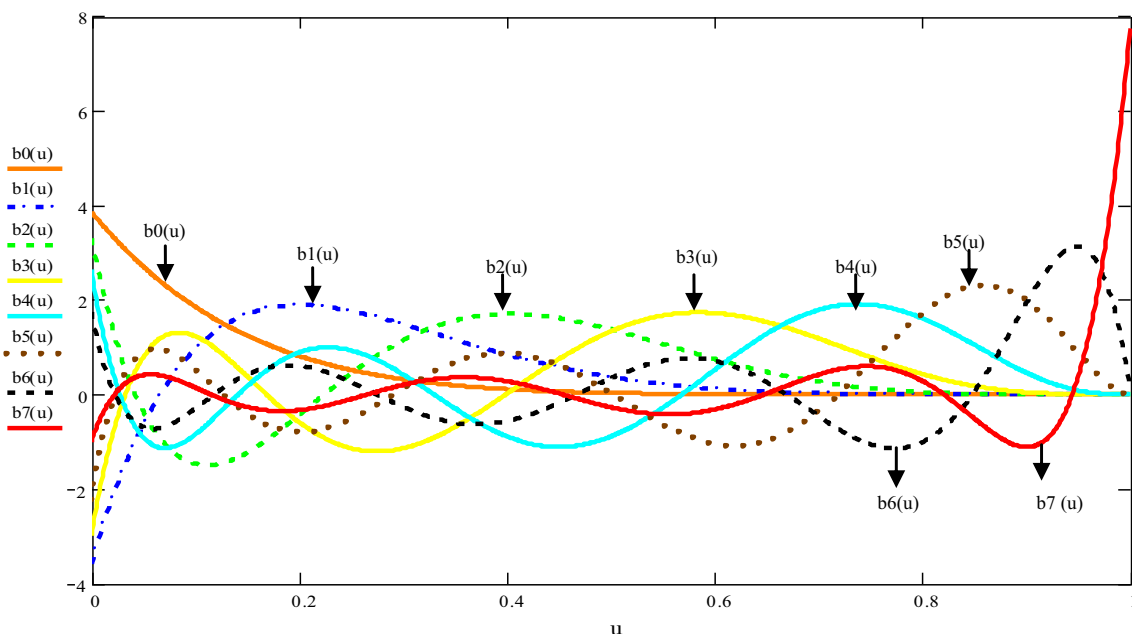


Fig. 1 Eight orthonormal Bernstein polynomials, for $N=7$

$$\Psi(u) = [\psi_{00}(u), \dots, \psi_{0N}(u); \psi_{10}(u), \dots, \psi_{1N}(u); \dots; \psi_{(2^k-1)0}(u), \dots, \psi_{(2^k-1)N}(u)]^T. \tag{8}$$

The solution of the system of generalized Abel integral equations

In this section, we are discussing the solution of the system of generalized Abel integral equations in Eq. (1) by using Bernstein polynomials orthonormal wavelet bases.

Now, let us take the unknown (emissivity) functions $\epsilon_1(u)$, $\epsilon_2(u)$ and the intensity functions $I_1(s), I_2(s)$ from Eq. (1) and approximates to this by using Eq. (6),

$$\begin{aligned} \epsilon_1(u) &= C_1^T \Psi(u), \quad \epsilon_2(u) = C_2^T \Psi(u); \\ I_1(s) &= F_1^T \Psi(s), \quad I_2(s) = F_2^T \Psi(s), \end{aligned} \tag{9}$$

where $C_1, C_2; F_1, F_2$ are coefficient matrices. Substituting these approximated values of functions from Eq. (9) and

$$\int_s^1 \frac{u^n du}{(u^\beta - s^\beta)^\alpha} = \frac{s^{1+n-\alpha\beta}}{\beta} \left[\frac{\Gamma[1-\alpha]\Gamma\left[\alpha - \left(\frac{1+n}{\beta}\right)\right]}{\Gamma\left[\frac{-n-1+\beta}{\beta}\right]} - \left(B_{s^\beta} \left[\alpha - \left(\frac{1+n}{\beta}\right), 1-\alpha \right] \right) \right]. \tag{11b}$$

taking $a = 0, b = 1$ in Eq. (1), we get

$$\begin{aligned} \rho_1(s)C_1^T \int_0^s \frac{u^{\beta-1}\Psi(u)du}{(s^\beta - u^\beta)^\alpha} + \rho_2(s)C_2^T \int_s^1 \frac{u^{\beta-1}\Psi(u)du}{(u^\beta - s^\beta)^\alpha} &= F_1^T \Psi(s) \\ \omega_1(s)C_1^T \int_s^1 \frac{u^{\beta-1}\Psi(u)du}{(u^\beta - s^\beta)^\alpha} + \omega_2(s)C_2^T \int_0^s \frac{u^{\beta-1}\Psi(u)du}{(s^\beta - u^\beta)^\alpha} &= F_2^T \Psi(s), \end{aligned} \tag{10}$$

The integrals in Eq. (10) involve evaluating integrals of the types $\int_0^s \frac{u^n du}{(s^\beta - u^\beta)^\alpha}$ and $\int_s^1 \frac{u^n du}{(u^\beta - s^\beta)^\alpha}$.

We calculate these integral using given recursive formulae,

$$\int_0^s \frac{u^n du}{(s^\beta - u^\beta)^\alpha} = \frac{\pi s^n (\beta/s)^{\alpha-1} (s^{\beta-1}\beta)^{-\alpha} \csc(\pi\alpha) \Gamma(n+1/\beta)}{\Gamma(\alpha)\Gamma(n+\beta-\beta\alpha+1/\beta)}, \tag{11a}$$

where $\Gamma(\cdot)$ represents the gamma function and $B_z(z, a, b)$ or $B_z(a, b)$ stands for the incomplete beta function which is defined by

$$B_z(a, b) \equiv \int_0^z t^{a-1}(1-t)^{b-1} dt,$$

$$\int_0^s \frac{u^{\beta-1}\Psi(u)}{(s^\beta - u^\beta)^\alpha} du = W_1\Psi(s), \quad \int_s^1 \frac{u^{\beta-1}\Psi(u)}{(u^\beta - s^\beta)^\alpha} du = W_2\Psi(s) \tag{12}$$

Here in Eq. (11b), we have $B_{s^\beta}(\alpha - n + 1/\beta, 1 - \alpha)$, which is expressed with the help of above function $B_z(a, b)$ as

$$B_{s^\beta} \left[\alpha - \left(\frac{1+n}{\beta} \right), 1 - \alpha \right] \equiv \int_0^{s^\beta} t^{\alpha - \left(\frac{1+n}{\beta} \right) - 1} (1-t)^{(1-\alpha)-1} dt.$$

where W_1 and W_2 are the almost Bernstein polynomial multi-wavelets operational matrix of integration [22, 23] of wavelet bases $\Psi(u)$ of order $2^k(N + 1) \times 2^k(N + 1)$.

The value of order eight matrices W_1 and W_2 for $N=7$ and $k=0$ ($\alpha = 1/3, \beta = 1$) is:

$$W_1 = \begin{bmatrix} 0.328623 & 0.421814 & 0.249677 & 0.230090 & 0.174416 & 0.151103 & 0.107665 & 0.064795 \\ -0.013906 & 0.307961 & 0.389789 & 0.214733 & 0.204112 & 0.144319 & 0.118830 & 0.062021 \\ 0.001558 & -0.027292 & 0.285000 & 0.353173 & 0.177834 & 0.175703 & 0.108464 & 0.071225 \\ -0.002993 & 0.004859 & -0.039681 & 0.259042 & 0.310580 & 0.139078 & 0.141380 & 0.059758 \\ 0.000082 & -0.001308 & 0.009575 & -0.050277 & 0.228978 & 0.259821 & 0.098334 & 0.087474 \\ -0.000029 & 0.000047 & 0.175703 & 0.139078 & 0.259821 & 0.192848 & -0.058880 & 0.023523 \\ 0.000013 & 0.000213 & -0.003516 & -0.007131 & 0.023177 & -0.05888 & 0.146459 & 0.109053 \\ -0.000005 & 0.000094 & -0.000685 & 0.003100 & -0.009843 & 0.023523 & -0.044944 & 0.075750 \end{bmatrix}$$

$$W_2 = \begin{bmatrix} 0.328623 & -0.013906 & 0.001558 & -0.002993 & 0.000082 & -0.000029 & 0.000013 & -0.000005 \\ 0.421814 & 0.307961 & -0.027292 & 0.004859 & -0.001308 & 0.000047 & -0.000213 & 0.000094 \\ 0.249677 & 0.389789 & 0.285000 & -0.039681 & 0.009957 & -0.003516 & 0.001559 & -0.000068 \\ 0.230090 & 0.214733 & 0.353173 & 0.259042 & -0.050277 & 0.016543 & -0.007131 & 0.003100 \\ 0.174416 & 0.204112 & 0.177834 & 0.31058 & 0.228978 & -0.057656 & 0.023177 & -0.009843 \\ 0.151103 & 0.144319 & 0.175703 & 0.139078 & 0.259821 & 0.192848 & -0.058880 & 0.023523 \\ 0.107665 & 0.118830 & 0.108464 & 0.141380 & 0.098334 & 0.196797 & 0.146459 & -0.044944 \\ 0.064795 & 0.062021 & 0.071225 & 0.059758 & 0.087474 & 0.052106 & 0.109053 & 0.075750 \end{bmatrix}$$

Now, by Eqs. (11a) and (11b) we have

Similarly, The value of order six matrices W_1 and W_2 for $N=5$ and $k=0$ ($\alpha = 1/2, \beta = 1$) is:

$$W_1 = \begin{bmatrix} 0.706694 & 0.669669 & 0.282085 & 0.284418 & 0.159798 & 0.111071 \\ -0.030444 & 0.669500 & 0.607355 & 0.227492 & 0.239991 & 0.092652 \\ 0.000236 & -0.0611950 & 0.622263 & 0.528185 & 0.168287 & 0.158927 \\ 0.000105 & 0.13697 & -0.090295 & 0.558931 & 0.465426 & 0.09712 \\ 0.000380 & -0.004750 & 0.028231 & -0.112400 & 0.465426 & 0.25556 \\ -0.000150 & 0.001866 & -0.010731 & 0.039044 & -0.10597 & 0.287359 \end{bmatrix},$$

$$W_2 = \begin{bmatrix} 0.706694 & -0.030444 & 0.000236 & 0.000105 & 0.000380 & -0.000150 \\ 0.669669 & 0.669500 & -0.0611950 & 0.13697 & -0.004750 & 0.001866 \\ 0.282085 & 0.607355 & 0.622263 & -0.090295 & 0.028231 & -0.010731 \\ 0.284418 & 0.227492 & 0.528185 & 0.558931 & -0.112400 & 0.039044 \\ 0.159798 & 0.239991 & 0.168287 & 0.421923 & 0.465426 & -0.10597 \\ 0.111071 & 0.092652 & 0.158927 & 0.09712 & 0.25556 & 0.287359 \end{bmatrix}.$$

The matrix W_2 can be calculated directly from W_1 , it is the transpose of W_1 , so it is easy to calculate them and one matrix can be written in the form of another matrix ($W_2 = W_1^T, W_1 = W_2^T$).

Now on substituting Eq. (12) in Eq. (10), we obtain

$$\left. \begin{aligned} \rho_1(s)C_1^T W_1 \Psi(s) + \rho_2(s)C_2^T W_2 \Psi(s) &= F_1^T \Psi(s) \\ \omega_1(s)C_1^T W_2 \Psi(s) + \omega_2(s)C_2^T W_1 \Psi(s) &= F_2^T \Psi(s) \end{aligned} \right\} \quad (13)$$

On simplifying we get

$$\left. \begin{aligned} \rho_1(s)C_1^T W_1 + \rho_2(s)C_2^T W_2 &= F_1^T \\ \omega_1(s)C_1^T W_2 + \omega_2(s)C_2^T W_1 &= F_2^T \end{aligned} \right\} \quad (13a)$$

Next, we solve the algebraic system in Eq. (13a), for the vectors C_1^T and C_2^T

$$\left. \begin{aligned} C_1^T &= [F_1^T \omega_2(s)W_1 - F_2^T \rho_2(s)W_2] [\rho_1(s)W_1 \omega_2(s)W_1 - \rho_2(s)W_2 \omega_1(s)W_2]^{-1}, \\ C_2^T &= [F_2^T \rho_1(s)W_1 - F_1^T \omega_1(s)W_2] [\rho_1(s)W_1 \omega_2(s)W_1 - \rho_2(s)W_2 \omega_1(s)W_2]^{-1} \end{aligned} \right\} \quad (13b)$$

We can also calculate the values of C_1^T and C_2^T for some special cases of the system given in Eq. (1),

(i) When the coefficient $\rho_1(s) = \omega_2(s)$ and $\rho_2(s) = \omega_1(s)$, then

On adding and subtracting equations of (13a), we get

$$\left. \begin{aligned} \rho_1(s)C_1^T W_1 + \rho_2(s)C_2^T W_2 + \omega_1(s)C_1^T W_2 + \omega_2(s)C_2^T W_1 &= F_1^T + F_2^T, \\ \rho_1(s)C_1^T W_1 + \rho_2(s)C_2^T W_2 - \omega_1(s)C_1^T W_2 - \omega_2(s)C_2^T W_1 &= F_1^T - F_2^T \end{aligned} \right\} \quad (13c)$$

Using approximations $\rho_1(s) = \omega_2(s)$ and $\rho_2(s) = \omega_1(s)$, Eq. (13c) becomes

$$\left. \begin{aligned} [C_1^T + C_2^T] \rho_1(s)W_1 + [C_1^T + C_2^T] \rho_2(s)W_2 &= F_1^T + F_2^T, \\ [C_1^T - C_2^T] \omega_2(s)W_1 - [C_1^T - C_2^T] \omega_1(s)W_2 &= F_1^T - F_2^T \end{aligned} \right\} \quad (13d)$$

Equation (13d) can be written in the following form

$$\left. \begin{aligned} [C_1 + C_2]^T &= [F_1 + F_2]^T [\rho_1(s)W_1 + \rho_2(s)W_2]^{-1} \\ [C_1 - C_2]^T &= [F_1 - F_2]^T [\omega_2(s)W_1 - \omega_1(s)W_2]^{-1} \end{aligned} \right\}, \quad (14)$$

Next, we solve the above algebraic system in Eq. (14) for the vectors C_1^T and C_2^T

$$\left. \begin{aligned} C_1^T &= \frac{1}{2} [[F_1 + F_2]^T [\rho_1(s)W_1 + \rho_2(s)W_2]^{-1} + [F_1 - F_2]^T [\omega_2(s)W_1 - \omega_1(s)W_2]^{-1}], \\ C_2^T &= \frac{1}{2} [[F_1 + F_2]^T [\rho_1(s)W_1 + \rho_2(s)W_2]^{-1} - [F_1 - F_2]^T [\omega_2(s)W_1 - \omega_1(s)W_2]^{-1}] \end{aligned} \right\} \quad (14a)$$

(ii) When the values of all coefficients of the system given in Eq. (1) are unity. Then using approximation $\rho_1(s) = \rho_2(s) = \omega_1(s) = \omega_2(s) = 1$, in Eq. (13c), we get

$$\left. \begin{aligned} [C_1 + C_2]^T &= [F_1 + F_2]^T [W_1 + W_2]^{-1} \\ [C_1 - C_2]^T &= [F_1 - F_2]^T [W_1 - W_2]^{-1} \end{aligned} \right\} \quad (14b)$$

Next, we solve the above algebraic system (14b) for the vectors C_1^T and C_2^T

$$\left. \begin{aligned} C_1^T &= \frac{1}{2} [[F_1 + F_2]^T [W_1 + W_2]^{-1} + [F_1 - F_2]^T [W_1 - W_2]^{-1}], \\ C_2^T &= \frac{1}{2} [[F_1 + F_2]^T [W_1 + W_2]^{-1} - [F_1 - F_2]^T [W_1 - W_2]^{-1}] \end{aligned} \right\} \quad (14c)$$

On substituting these values of the vectors C_1^T and C_2^T [for the general case from Eq. (13b), for the special case (i) from Eq. (14a) and special case (ii) from Eq. (14c)] in Eq. (9), we get the following approximate solutions

$$\varepsilon_1(u) = C_1^T \Psi(u); \varepsilon_2(u) = C_2^T \Psi(u). \quad (15)$$

See ‘‘Appendix 2’’.

Convergence of the wavelet bases

In this section, we discuss a lemma and theorem that supports the absolute error of the proposed method and also presents an error analysis of the proposed method.

Lemma 1

(See [24]) Let the function $\varepsilon(u) \in C^n[0, 1]$, be a collection of all real-valued n times continuously differentiable functions. The mean error bound of approximation in Eq. (6) is

$$\|C^T \Psi(u) - \varepsilon(u)\| \leq \frac{2}{4^n 2^{nk} n!} \sup_{x \in [0,1]} |\varepsilon^{(n)}(u)|. \quad (16)$$

Proof Let us divide the existing interval $[0, 1]$ into subintervals $[m/2^k, m+1/2^k] = I_{m,k}$ (say), on which the restriction

of $C^T \Psi(u)$ to one such subinterval $I_{m,k}$ is the polynomial of order n that interpolates $\varepsilon(u)$ with the minimum mean error. Following which, we employ the maximum error estimation

for the polynomial which interpolates $\varepsilon(u)$ at Chebyshev nodes, of order n . The interpolation polynomial of $C^T\Psi(u)$ is that unique polynomial that has a value $\varepsilon(u_i)$ at every point u_i . The interpolation error at u is given by [24],

$$\varepsilon(u) - C^T\Psi(u) = \frac{\varepsilon^{(n)}(\xi)}{n!} \prod_{i=1}^n (u - u_i)$$

for some ξ (depending on u) in $[a, b]$, so it is obvious to minimize $\sup_{u \in [0, 1]} \left| \prod_{i=1}^n (u - u_i) \right|$ for better convergence as $n \rightarrow \infty$, here product represents in the form of monic polynomials. It can be demonstrated that the maximum norm of such polynomial is bounded below by 2^{1-n} . This bound is obtained by scaled Bernstein polynomials $2^{1-n}B_n$, which are monic as well. Thus, for an arbitrary interval $[a, b]$ the roots of the given polynomial are the interpolation Chebyshev nodes u_i , and the error satisfies the following equation

$$|\varepsilon(u) - C^T\Psi(u)| \leq \frac{2^{1-n}}{n!} \left(\frac{b-a}{2}\right)^n \sup_{\xi \in [a,b]} |\varepsilon^{(n)}(\xi)| \tag{17a}$$

□

The left side of Eq. (16);

$$\|C^T\Psi(u) - \varepsilon(u)\|^2 = \int_0^1 [C^T\Psi(u) - \varepsilon(u)]^2 du$$

$$\|C^T\Psi - \varepsilon\|^2 = \sum_k \int_{I_{m,k}} [C^T\Psi(u) - \varepsilon(u)]^2 du$$

Using Eq. (17a) and $I_{m,k} = [m/2^k, m+1/2^k]$ we get

$$\|C^T\Psi - \varepsilon\|^2 \leq \int_0^1 \left(\frac{2^{1-nk}}{4^n n!} \sup_{u \in [0,1]} |\varepsilon^{(n)}(u)| \right)^2 du$$

$$\|C^T\Psi - \varepsilon\|^2 \leq \left(\frac{2}{4^n 2^{nk} n!} \sup_{u \in [0,1]} |\varepsilon^{(n)}(u)| \right)^2 \tag{17b}$$

The square root of the Eq. (17b) will give the upper bound of the given approximation in Eq. (6). The approximation error of the function $\varepsilon(u)$ rapidly decays like $1/2^{nk}$. These bounds of the error obtained are governed by the term $1/(2^{2n+nk-1}n!)$, which varies inversely with values of k and n and minimizes to zero as values of k and n increase significantly. On the contrary, in classical orthogonal bases such as Chebyshev, Legendre and Fourier, it depends on $1/n!$. Here, the two arguments n and k , in the basis are the two degrees of freedom for the B-polynomial wavelet bases, which help

in the accuracy of the introduced method. This is the advantage of the proposed method.

Theorem 1 (Ref. [25]) *Suppose that the known functions in the system of generalized Abel integral equations are real $n + 1$ times continuously differentiable functions on the bounded interval $[0, 1]$ and $\sum_{i=0}^{\infty} c_i \Psi(u)$ be the infinite series expansion of exact solution $\varepsilon(u)$, in the form of Bernstein polynomials orthonormal wavelet bases and $\varepsilon_n(u)$ denotes its truncation such as $C^T\Psi(u)$ and similarly, $\tilde{\varepsilon}(u)$ is the infinite expansion of the approximate solution and $\tilde{\varepsilon}_n(u)$ is the truncated part of $\tilde{\varepsilon}(u)$, taken as $\tilde{C}^T\Psi(u)$, then there exist the real numbers λ_1 and λ_2 such that*

$$\Delta\varepsilon(u) = \|\varepsilon(u) - \tilde{\varepsilon}_n(u)\|_2 \leq \lambda_1 S_{n;k} + \lambda_2 \|C - \tilde{C}\|_2 \tag{18}$$

where

$$C = [c_{00}, c_{01}, \dots, c_{0N}, c_{10}, \dots, c_{1N}, \dots, c_{(2^k-1)0}, \dots, c_{(2^k-1)N}]^T;$$

$$\tilde{C} = [\tilde{c}_{00}, \tilde{c}_{01}, \dots, \tilde{c}_{0N}, \tilde{c}_{10}, \dots, \tilde{c}_{1N}, \dots, \tilde{c}_{(2^k-1)0}, \dots, \tilde{c}_{(2^k-1)N}]^T$$

and

$$S_{n;k} = \left(\frac{1}{2^{n.k+2n-1}n!} \right) \sup_{\xi \in [a,b]} |\varepsilon^{(n)}(\xi)|.$$

Proof Let us take the truncated series $\varepsilon_n(u)$ and $\tilde{\varepsilon}_n(u)$ are in $R_n[u]$ (where $R_n[u]$ is the space of real-valued polynomials of degree less than equal to the space of real-valued polynomials of degree less than equal to n), $\varepsilon_n(u)$ is the best approximation of $\varepsilon(u)$ in $R_n[u]$, then

$$\begin{aligned} \|\varepsilon(u) - \tilde{\varepsilon}_n(u)\|_2 &= \|\varepsilon(u) - \varepsilon_n(u) + \varepsilon_n(u) - \tilde{\varepsilon}_n(u)\|_2 \\ &\leq \|\varepsilon(u) - \varepsilon_n(u)\|_2 + \|\varepsilon_n(u) - \tilde{\varepsilon}_n(u)\|_2. \end{aligned} \tag{19}$$

Now, the first part of the right-hand side of Eq. (19), yields

$$\|\varepsilon(u) - \varepsilon_n(u)\|_2 = \int_0^1 \left[|\varepsilon(u) - \varepsilon_n(u)|^2 du \right]^{1/2}$$

using Lemma 1, we get

$$\leq \left[\int_0^1 (S_{n;k})^2 du \right]^{1/2}$$

$$\|\varepsilon(u) - \varepsilon_n(u)\|_2 \leq S_{n;k}; \text{ so } \lambda_1 = 1. \tag{20}$$

Also, the second part of the right-hand side of Eq. (19), yields

$$\|\varepsilon_n(u) - \tilde{\varepsilon}_n(u)\|_2 = \left[\int_0^1 \left| \sum_{i=0}^n (C_i - \tilde{C}_i) \Psi_i(u) \right|^2 du \right]^{1/2}$$

i.e.,

$$(\|\varepsilon_n(u) - \tilde{\varepsilon}_n(u)\|_2)^2 = \int_0^1 \left| \sum_{i=0}^n (C_i - \tilde{C}_i) \Psi_i(u) \right|^2 du. \tag{21}$$

□

Now, we use the generalized triangular inequality in the right-hand side of Eq. (21), such as

$$\begin{aligned} & \int_0^1 \left| \sum_{i=0}^n (C_i - \tilde{C}_i) \Psi_i(u) \right|^2 du \\ & \leq \int_0^1 \left(\sum_{i=0}^n |C_i - \tilde{C}_i| |\Psi_i(u)| \right)^2 du \\ & = \int_0^1 \left[\sum_{i=j=0}^n |C_i - \tilde{C}_i|^2 |\Psi_i(u)|^2 + \sum_{i \neq j=0}^n |C_i - \tilde{C}_i| |C_j - \tilde{C}_j| |\Psi_i(u)| |\Psi_j(u)| \right] du \\ & = \sum_{i=j=0}^n |C_i - \tilde{C}_i|^2 \int_0^1 |\Psi_i(u)|^2 du + \sum_{i \neq j=0}^n |C_i - \tilde{C}_i| |C_j - \tilde{C}_j| \int_0^1 |\Psi_i(u)| |\Psi_j(u)| du \end{aligned}$$

using orthonormality of Bernstein polynomial multiwavelets

$$= \sum_{i=0}^n |C_i - \tilde{C}_i|^2. \tag{22}$$

Next, by substituting Eq. (22) in Eq. (21) we get,

$$\|\varepsilon_n(u) - \tilde{\varepsilon}_n(u)\|_2 \leq \|C - \tilde{C}\|. \tag{23}$$

We substituted values from Eq. (20) and Eq. (23) in Eq. (18) and concluded that it holds valid for

$$\lambda_1 = 1; \lambda_2 = 1.$$

Hence, as illustrated, $\Delta\varepsilon(u)$ decreases as $n \rightarrow \infty$.

Illustrative example

The estimated solution $\varepsilon(u)$ (emissivity) cannot be calculated exactly if the data function $I(s)$ is given with very small or high-frequency errors. These errors in the data

function can occur from experimental errors which results into large errors in emissivity since differentiation of the measured data is required in these formulae, that's why the stable numerical techniques become vital, but in the proposed method there is no need of the differentiation of data function. Thus, we have suggested a new stable numerical technique for the solution of the system given in Eq. (1). The stability of the proposed method is showing for a system by adding noise μ in $I(s)$ and presented the convergence of the proposed method by calculating the pointwise error. Some suitable illustrative examples with figures are given to show the stability and accuracy of the introduced method for the known system even with particular noise μ .

Next, the exactness of the proposed method is shown by

calculating the absolute error $\Delta\varepsilon(u_i)$ with the help of Theorem 1, such that

$$\Delta\varepsilon(u_i) = |\varepsilon(u_i) - \tilde{\varepsilon}_n(u_i)|, \tag{24}$$

where $\tilde{\varepsilon}_n(u_i)$ and $\varepsilon(u_i)$ are the estimated solution and exact solutions calculated at the corresponding point u_i , respectively. Also, $I(s)$ and $I^\mu(s)$ represent the exact and noisy profiles, respectively, where $I^\mu(s)$ is obtained by adding a noise μ to $I(s)$, i.e., $I^\mu(s_i) = I(s_i) + \mu\theta_i$ where θ_i stands for the uniform random variable which takes values in $[-1, 1]$, $s_i = i\mu$, $i = 1, \dots, \tilde{N}$, $\tilde{N}\mu = 1$ and $\text{Max}_{1 \leq i \leq \tilde{N}} |I_i^\mu(s) - I_i(s)| \leq \mu$.

Now, using Eqs. (14a) and (15) the reconstructed emissivities ${}^\mu\tilde{\varepsilon}_i$ are obtained with noise term μ in intensity profile under the condition $\rho_1(s) = \omega_2(s)$ and $\rho_2(s) = \omega_1(s)$, are given as

$$\begin{aligned}
 {}^\mu \tilde{\varepsilon}_1(u) &\approx \frac{1}{2} \left[({}^\mu F_1 + {}^\mu F_2)^T (\rho_1(s)W_1 + \rho_2(s)W_2)^{-1} + ({}^\mu F_1 - {}^\mu F_2)^T (\omega_2(s)W_1 - \omega_1(s)W_2)^{-1} \right] \Psi(u), \\
 {}^\mu \tilde{\varepsilon}_2(u) &\approx \frac{1}{2} \left[({}^\mu F_1 + {}^\mu F_2)^T (\rho_1(s)W_1 + \rho_2(s)W_2)^{-1} + ({}^\mu F_1 - {}^\mu F_2)^T (\omega_2(s)W_1 - \omega_1(s)W_2)^{-1} \right] \Psi(u)
 \end{aligned}
 \tag{25}$$

where ${}^\mu I_i(s)$ and $I_i(s)$ are known functions ($i = 1, 2$), and they are obtained from the following equations:

$${}^\mu I_i(s) = I_i(s) + \mu \theta_i \approx {}^\mu F_i^T \Psi(u)$$

and

$$I_i(s) \approx F_i^T \Psi(u).$$

Hence from Eqs. (15) and (25)

$$\begin{aligned}
 {}^\mu \tilde{\varepsilon}_1(u) - \tilde{\varepsilon}_1(u) &= \left[\frac{1}{2} \left\{ ({}^\mu F_1 + {}^\mu F_2)^T (\rho_1(s)W_1 + \rho_2(s)W_2)^{-1} \right. \right. \\
 &\quad \left. \left. + ({}^\mu F_1 - {}^\mu F_2)^T (\omega_2(s)W_1 - \omega_1(s)W_2)^{-1} \right\} \Psi(u) \right] \\
 &\quad - \left[\frac{1}{2} \left\{ (F_1 + F_2)^T (\rho_1(s)W_1 + \rho_2(s)W_2)^{-1} \right. \right. \\
 &\quad \left. \left. + (F_1 - F_2)^T (\omega_2(s)W_1 - \omega_1(s)W_2)^{-1} \right\} \Psi(u) \right]
 \end{aligned}$$

i.e.,

$$\begin{aligned}
 {}^\mu \tilde{\varepsilon}_1(u) - \tilde{\varepsilon}_1(u) &= \frac{1}{2} \left[(H_1^T + H_2^T) (\rho_1(s)W_1 + \rho_2(s)W_2)^{-1} \right. \\
 &\quad \left. + (H_1^T - H_2^T) (\omega_1(s)W_1 - \omega_2(s)W_2)^{-1} \right] \Psi(u),
 \end{aligned}$$

where $H_1^T = {}^\mu F_1^T - F_1^T$, $H_2^T = {}^\mu F_2^T - F_2^T$ and

$$\begin{aligned}
 \| {}^\mu \tilde{\varepsilon}_1(u) - \tilde{\varepsilon}_1(u) \|_2 &\leq \frac{1}{2} \left(\| H_1^T + H_2^T \| \| [\rho_1(s)W_1 + \rho_2(s)W_2]^{-1} \| \right. \\
 &\quad \left. + \| H_1^T - H_2^T \| \| [\omega_2(s)W_1 - \omega_1(s)W_2]^{-1} \| \right) \| \Psi(u) \|
 \end{aligned}$$

Similarly, from Eqs. (15) and (25), we get

$$\begin{aligned}
 \| {}^\mu \tilde{\varepsilon}_2(u) - \tilde{\varepsilon}_2(u) \|_2 &\leq \frac{1}{2} \left(\| H_1^T + H_2^T \| \| [\rho_1(s)W_1 + \rho_2(s)W_2]^{-1} \| \right. \\
 &\quad \left. - \| H_1^T - H_2^T \| \| [\omega_2(s)W_1 - \omega_1(s)W_2]^{-1} \| \right) \| \Psi(u) \|.
 \end{aligned}$$

Setting,

$$h_1(u) = {}^\mu \tilde{\varepsilon}_1(u) - \tilde{\varepsilon}_1(u)$$

and

$$h_2(u) = {}^\mu \tilde{\varepsilon}_2(u) - \tilde{\varepsilon}_2(u),$$

then $h_1(u)$ and $h_2(u)$ reflect the noise reduction capability [23] of the method, which is shown in Figs. 6 and 7, for example, 1. The general behavior of noise reduction is the same irrespective of the value of μ .

Example 1 In the first example, consider Eq. (1) with $\rho_1(s)$, $\rho_2(s)$; $\omega_1(s)$ and $\omega_2(s)$ are unity and $\beta = 1$, $\alpha = 1/3$ for the pairs:

$$\begin{aligned}
 I_1(s) &= e^s \left[\Gamma\left(\frac{2}{3}\right) - \Gamma\left(\frac{2}{3}, s\right) \right] \\
 &\quad + \frac{e^{2s}(1-s)^{\frac{2}{3}} \left[\Gamma\left(\frac{2}{3}\right) - \Gamma\left(\frac{2}{3}, s-1\right) \right]}{2^{\frac{2}{3}}(s-1)^{\frac{2}{3}}} \\
 I_2(s) &= \frac{e^s(1-s)^{\frac{2}{3}} \left[\Gamma\left(\frac{2}{3}\right) - \Gamma\left(\frac{2}{3}, s-1\right) \right]}{(s-1)^{\frac{2}{3}}} \\
 &\quad + \frac{e^{2s}(1-s)^{\frac{2}{3}} \left[\Gamma\left(\frac{2}{3}\right) - \Gamma\left(\frac{2}{3}, s-1\right) \right]}{2^{\frac{2}{3}}},
 \end{aligned}
 \tag{26}$$

where $\Gamma(\cdot)$ represents the gamma functions and

$$\varepsilon_1(u) = e^u, \quad \varepsilon_2(u) = e^{2u},$$

are exact solutions of Eq. (1) for the above values of $I_1(s)$, $I_2(s)$ and Eqs. (14c) and (15) provide the desired approximate solutions

$$\tilde{\varepsilon}_1(u) = \tilde{C}_1^T \Psi(u), \quad \tilde{\varepsilon}_2(u) = \tilde{C}_2^T \Psi(u).$$

Here, the Bernstein polynomials orthonormal wavelet bases are taking for $k = 0, 1$; $N = 7$ and apply the introduced method, to get the approximate solutions of Eq. (26), which are shown in Table 1. Now, the associated absolute errors without noise are depicted by

$$\begin{aligned}
 E_1(u) &= |\varepsilon_1(u) - \tilde{\varepsilon}_1(u)| \\
 E_2(u) &= |\varepsilon_2(u) - \tilde{\varepsilon}_2(u)|,
 \end{aligned}$$

which are shown in Figs. 2 and 3, respectively, for dilation parameter $k = 0$ and $k = 1$. The comparison of absolute errors $E_3(u)$, $E_4(u)$ for the noise level $\mu_1 = 0.001$ and $E_5(u)$, $E_6(u)$ at the noise level $\mu_2 = 0.002$, respectively, for $k = 0$ and $k = 1$ are shown in Figs. 4 and 5. The stability of the proposed method is shown by calculating the noise reducing capability $h_1(u)$ and $h_2(u)$ which are shown in Figs. 6 and 7 for example 1, similarly we can calculate noise reducing capability for other examples.

Table 1 Approximate and exact solution of example 1

u_i	Exact solutions		Approximate solutions (for $k=0$)		Approximate solutions (for $k=1$)	
	$\varepsilon_1(u)$	$\varepsilon_2(u)$	$\tilde{\varepsilon}_1(u)$	$\tilde{\varepsilon}_2(u)$	$\tilde{\varepsilon}_1(u)$	$\tilde{\varepsilon}_2(u)$
0.0	1.000000	1.000000	1.000270	1.000281	0.997975	0.998116
0.2	1.221403	1.491825	1.221409	1.491827	1.22118	1.491657
0.4	1.491825	2.225541	1.49181	2.225527	1.488941	2.222198
0.6	1.822119	3.320117	1.822141	3.320135	1.821359	3.319568
0.8	2.225541	4.953032	2.225528	4.953012	2.225257	4.952939
0.9	2.459603	6.049647	2.459633	6.049662	2.459723	6.049632

Fig. 2 Comparison of the absolute errors with noise $\mu = 0$ in example 1, for $k = 0$

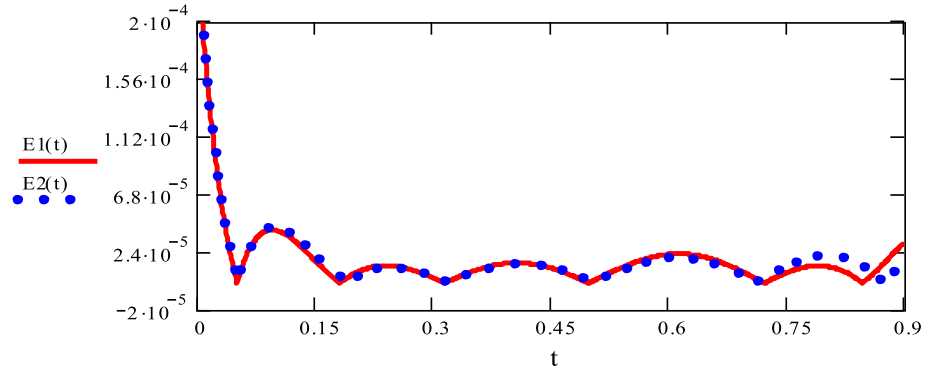
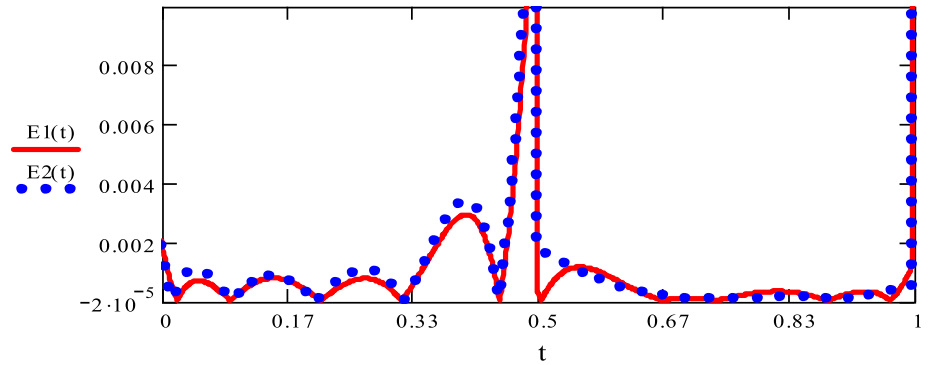


Fig. 3 Comparison of the absolute errors with noise $\mu = 0$ in example 1, for $k = 1$



Example 2 Let us consider Eq. (1) with $\rho_1(s) = (s^2 + 1)$, $\rho_2(s) = \frac{(s+1)}{4}$; $\omega_1(s) = \frac{s^2}{2}$, $\omega_2(s) = 2 - s$ and $\alpha = 1/2, \beta = 1$ for the pairs [14]:

$$\begin{aligned}
 I_1(s) &= \frac{16}{15}s^{5/2}(1 + s^2) + \frac{1}{70}(s + 1)\sqrt{1 - s}[5 + 2s(3 + 4s + 8s^2)], \\
 I_2(s) &= \frac{16}{35}s^{11/2} + (2 - s)\left[\frac{2}{15}\sqrt{1 - s}(3 + 4s + 8s^2)\right]
 \end{aligned}
 \tag{27}$$

there exist an analytical solution of Eq. (1) for the above $I_1(s), I_2(s)$, like as

$$\varepsilon_1(u) = u^2; \quad \varepsilon_2(u) = u^3.$$

Here, we applied the proposed method similar to the example 1 for $N=5$ and $k=0$ to get the desired approximate solution

$$\tilde{\varepsilon}_1(u) = \tilde{C}_1^T \Psi(u), \quad \tilde{\varepsilon}_2(u) = \tilde{C}_2^T \Psi(u).$$

Now, the comparison of the approximated solution for the proposed method and the given method in Ref. [14] is shown in Table 2, even less number of polynomials taken but achieves better results with higher accuracy are obtained in the present method. Next, the absolute errors $E_1(u), E_2(u)$ for the proposed method are of order 10^{-5} as shown in Fig. 8. Whereas, the comparison of absolute errors $E_3(u), E_4(u)$ for the noise level $\mu_1 = 0.001$, and $E_5(u), E_6(u)$ at the noise level

Fig. 4 Comparison of absolute errors with noises $\mu_1 = 0.001, \mu_2 = 0.002$ in example 1, for $k=0$

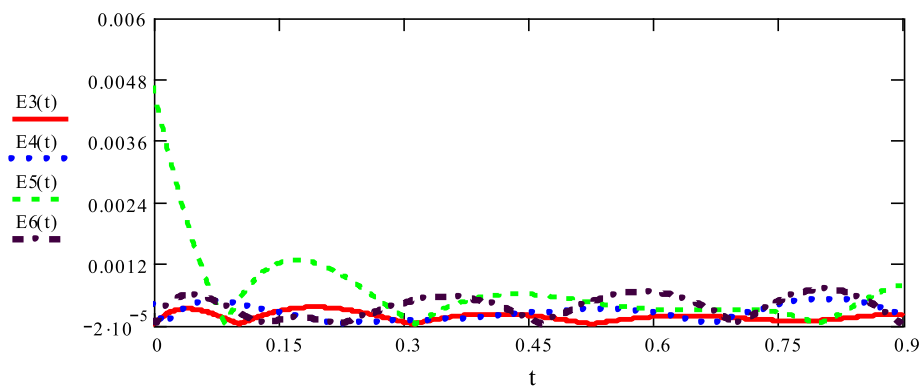


Fig. 5 Comparison of absolute errors with noises $\mu_1=0.001, \mu_2=0.002$ in example 1, for $k=1$

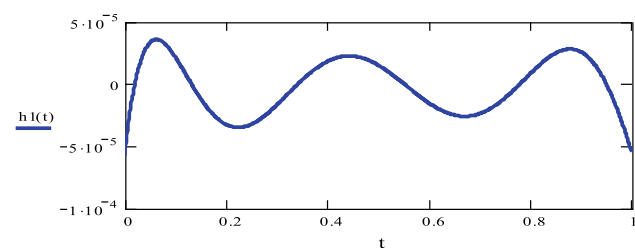
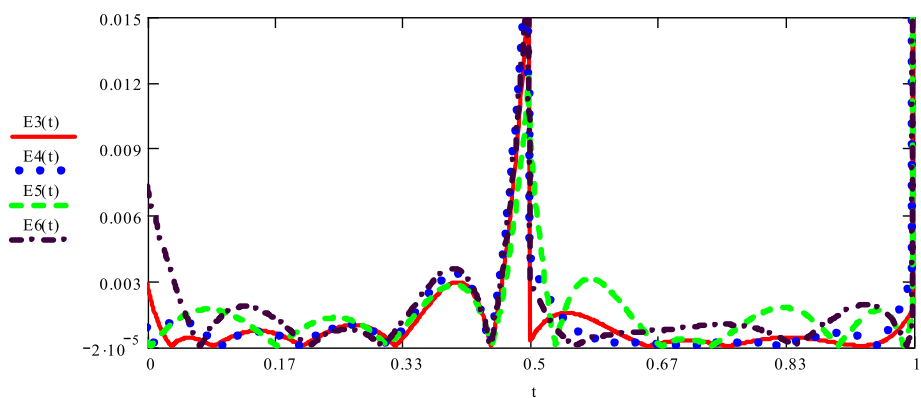


Fig. 6 Noise reduction $h_1(u)$ for the solution function $\tilde{\epsilon}_1(u)$ in example 1

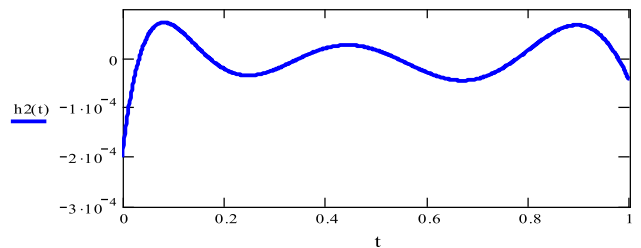
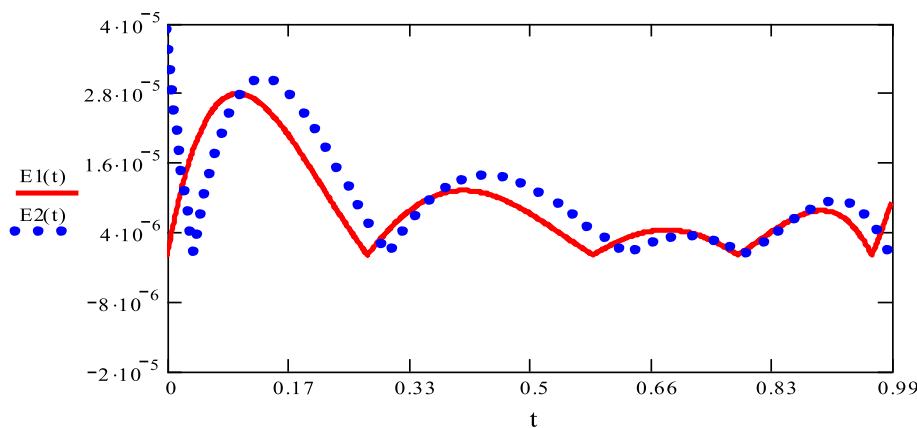


Fig. 7 Noise reduction $h_2(u)$ for the solution function $\tilde{\epsilon}_2(u)$ in example 1

Table 2 Comparison between the proposed method and Bernstein polynomial method [14]

u_i	Exact solutions		Approximate solutions by the proposed method (for $M = 5, k = 0$)		Approximate solutions by Bernstein polynomials [14] (for $M=8$)	
	$\epsilon_1(u)$	$\epsilon_2(u)$	$\tilde{\epsilon}_1(u)$	$\tilde{\epsilon}_2(u)$	$\tilde{\epsilon}_1(u)$	$\tilde{\epsilon}_2(u)$
0.0	0	0	0.000006	0.000047	0.000000	0.000000
0.2	0.04	0.008	0.039986	0.007976	0.040019	0.008019
0.4	0.16	0.064	0.160012	0.064013	0.160049	0.064023
0.6	0.36	0.216	0.359999	0.216002	0.359974	0.215971
0.8	0.64	0.512	0.640002	0.512000	0.639978	0.511841

Fig. 8 Comparison of absolute errors in example 2, for $k=0$



$\mu_2=0.002$, respectively, for $k=0$ and $k=1$ can be obtained to the similar of example 1.

Example 3 In this example, we consider Eq. (1) with $\rho_1(s) = \rho_2(s) = 1$; $\omega_1(s) = \omega_2(s) = 1$ and $\alpha = 1/2, \beta = 2$ for the pairs

$$\begin{aligned}
 I_1(s) &= \frac{4s^{3/2}}{3} + e^s \sqrt{\pi} \operatorname{erf}(\sqrt{s}) + \frac{2}{15} \sqrt{1-s}(3 + 4s + 8s^2), \\
 I_2(s) &= \frac{16s^{5/2}}{15} + \frac{2(1 + s - 2s^2)}{3\sqrt{s-1}} + \frac{e^s \sqrt{\pi - \pi s} \operatorname{erf}(\sqrt{s-1})}{\sqrt{s-1}}
 \end{aligned}
 \tag{28}$$

with the exact solution

$$\varepsilon_1(u) = e^u + u, \varepsilon_2(u) = u^2,$$

where

$$\operatorname{erf}(s) = \frac{2}{\sqrt{\pi}} \int_0^s e^{-t^2} dt.$$

and its approximate solutions $\tilde{\varepsilon}_1(u), \tilde{\varepsilon}_2(u)$ are free from noise, which is presented in Table 3, for $N=5, k=0$ by the same approach used in the above examples. Now, the absolute errors $E_1(u), E_2(u)$ associated with example 3 are obtained similar to the first example, and it is shown in Fig. 9.

Next, the comparison to the proposed method for this example is shown in Table 3 from the exact solution.

Conclusions

The system investigated in this paper holds substantial significance in the determination of intensity and emissivity of the plasma spectroscopy model. Our technique demonstrates

the comparison between solutions for two different dilation parameters, i.e., $k=0$ and $k=1$. The stability with relevancy to the data is restored, and a favorable result is obtained, even for small sample intervals with high noise in the data. The selection of a small number of orthonormal polynomials (as shown for $n=5$ and $n=7$) makes the method easy and straightforward. The error bound obtained demonstrates that a higher degree of convergence is achieved even in the case of an infinite system as compared to the other method in Ref. [25]. This method [25] failed for an infinite system as the series obtained from the difference of truncated functions $\varepsilon_n(u)$ and $\tilde{\varepsilon}_n(u)$

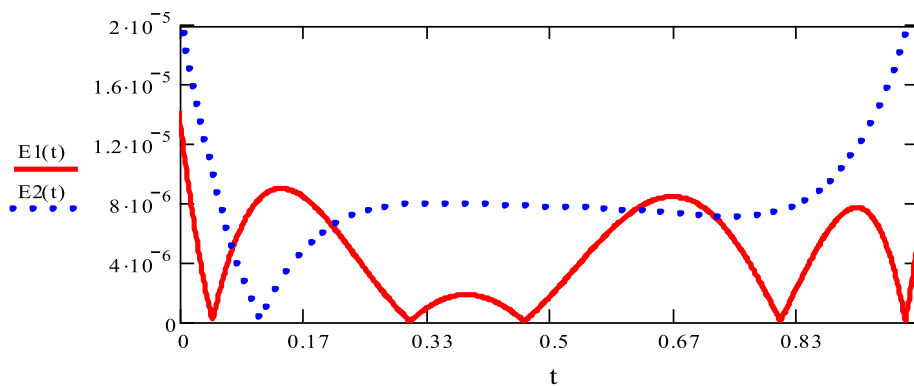
$$\|\varepsilon_n(u) - \tilde{\varepsilon}_n(u)\|_2 \leq \|C - \tilde{C}\|_2 \left(l \sum_{i=0}^n \frac{1}{2i+1} \right)^{\frac{1}{2}}$$

is a diverging series as $n \rightarrow \infty$. Hence, it gives a weaker bound. But in the proposed method, it is less than or equal to $\|C - \tilde{C}\|_2$, which holds for every value of n , so it converges slowly even in the case of $n \rightarrow \infty$.

Table 3 Comparison between the exact and proposed solution

u_i	Exact solution		Approximate solutions by the proposed method (for $M=5, k=0$)	
	$\varepsilon_1(u)$	$\varepsilon_2(u)$	$\tilde{\varepsilon}_1(u)$	$\tilde{\varepsilon}_2(u)$
0.0	1.000000	0.000000	1.000014	-0.000022
0.1	1.205171	0.010000	1.205163	0.009999
0.2	1.421403	0.040000	1.421396	0.040006
0.3	1.649859	0.900000	1.649858	0.090008
0.4	1.891825	0.160000	1.891826	0.160008
0.5	2.148721	0.250000	2.148720	0.250008
0.6	2.422119	0.360000	2.422112	0.360008
0.7	2.713753	0.490000	2.713745	0.490007
0.8	3.025541	0.640000	3.025540	0.640007
0.9	3.359603	0.810000	3.359610	0.810010

Fig. 9 Comparison of absolute errors in example 3, for $k=0$



Acknowledgements We would like to thank anonymous reviewers whose critical comments and valuable suggestions helped for improvement of the manuscript. The first author Shweta Pandey is working as a Ph.D. Scholar under the guidance of Dr. S. R. Verma Assistant Professor, Department of Mathematics and Statistics, Gurukula Kangri Vishwavidyalaya, Haridwar and thankful to him for all his support and guidance.

Appendix 1: Gram–Schmidt process for finding Orthonormal Bernstein Polynomials

The Bernstein polynomial of degree N is $B_{i,N}(y)$

Step 1 $b_0(y) := \frac{B_{0,N}(y)}{\|B_{0,N}(y)\|}$

Step 2 For $i = 1$ to N

$$C_{i,N}(y) := B_{i,N}(y) - \frac{\langle B_{i,N}(y), C_{i-1,N}(y) \rangle}{\|C_{i-1,N}(y)\|} * C_{i-1,N}(y) - \frac{\langle B_{i,N}(y), C_{i-2,N}(y) \rangle}{\|C_{i-2,N}(y)\|} * C_{i-2,N}(y) \dots - \frac{\langle B_{i,N}(y), B_{0,N}(y) \rangle}{\|B_{0,N}(y)\|} * B_{0,N}(y)$$

Step 3 $b_i(y) := \frac{C_{i,N}(y)}{\|C_{i,N}(y)\|}$

$b_i(y)$ is the required Bernstein polynomial. Here, $\langle p(y), q(y) \rangle$ represents the inner product of $p(y)$ and $q(y)$ in the Hilbert space $L^2(R)$ and $\|\xi(y)\|$ is the L^2 norm of the given function $\xi(y)$.

Appendix 2: Algorithm for the numerical method

1. Obtain the orthonormalized version $b_n(u)$ of Bernstein polynomials $B_{i,n}(u)$.
2. Evaluate $\psi_{mn}(u)$ on the interval $[0, 1)$ using $b_n(u)$.
3. Manipulate operational matrices W_1 and W_2 .

4. Find determinant $(W_1 + W_2)$ and determinant $(W_1 - W_2)$, if it is nonzero then we proceed further and go to step 5 otherwise the solution $\varepsilon_1(u)$ and $\varepsilon_2(u)$ cannot be computed.
5. Manipulate matrices F_1^T and F_2^T .
6. Calculate values of C_1^T and C_2^T for different cases accordingly

In general case

$$C_1^T = [F_1^T \omega_2(s)W_1 - F_2^T \rho_2(s)W_2] \times [\rho_1(s)W_1 \omega_2(s)W_1 - \rho_2(s)W_2 \omega_1(s)W_2]^{-1},$$

$$C_2^T = [F_2^T \rho_1(s)W_1 - F_1^T \omega_1(s)W_2] \times [\rho_1(s)W_1 \omega_2(s)W_1 - \rho_2(s)W_2 \omega_1(s)W_2]^{-1}$$

For particular case (i) when $\rho_1(s) = \omega_2(s)$ and $\rho_2(s) = \omega_1(s)$,

$$C_1^T = \frac{1}{2} [[F_1 + F_2]^T [\rho_1(s)W_1 + \rho_2(s)W_2]^{-1} + [F_1 - F_2]^T [\omega_2(s)W_1 - \omega_1(s)W_2]^{-1}],$$

$$C_2^T = \frac{1}{2} [[F_1 + F_2]^T [\rho_1(s)W_1 + \rho_2(s)W_2]^{-1} - [F_1 - F_2]^T [\omega_2(s)W_1 - \omega_1(s)W_2]^{-1}]$$

For particular case (ii) when $\rho_1(s) = \rho_2(s) = \omega_1(s) = \omega_2(s) = 1$,

$$C_1^T = \frac{1}{2} [[F_1 + F_2]^T [W_1 + W_2]^{-1} + [F_1 - F_2]^T [W_1 - W_2]^{-1}],$$

$$C_2^T = \frac{1}{2} [[F_1 + F_2]^T [W_1 + W_2]^{-1} - [F_1 - F_2]^T [W_1 - W_2]^{-1}].$$

7. Put values of C_1^T and C_2^T from step 6 to get the desired solution is $\varepsilon_1(u) = C_1^T \Psi(u)$; $\varepsilon_2(u) = C_2^T \Psi(u)$.

References

- De, S., Mandal, B.N., Chakrabarti, A.: Use of Abel integral equations in water wave scattering by two surface-piercing barriers. *Wave Motion* **47**(5), 279–288 (2010)
- Andanson, P., Cheminat, B., Halbique, A.M.: Numerical solution of the Abel integral equation: application to plasma spectroscopy. *J. Phys. D Appl. Phys.* **11**(3), 209 (1978)
- Gorenflo, R., Vessella, S.: *Abel integral equations: analysis and applications*, pp. 23–37, 61–63. Springer, Berlin (1991)
- Aben, H., Ainola, L., Errapart, A.: Application of the Abel inversion in case of a tensor field. *Inverse Probl. Sci. Eng.* **18**(2), 241–249 (2010)
- Asaki, T.J., Campbell, P.R., Chartrand, R., Powell, C.E., Vixie, K.R., Wohlberg, B.E.: Abel inversion using total variation regularization: applications. *Inverse Probl. Sci. Eng.* **14**(8), 873–885 (2006)
- Maleknejad, K., Sohrabi, S.: Numerical solution of Fredholm integral equations of the first kind by using Legendre wavelets. *Appl. Math. Comput.* **186**(1), 836–843 (2007)
- Maleknejad, K., Mirzaee, F.: Using rationalized Haar wavelet for solving linear integral equations. *Appl. Math. Comput.* **160**(2), 579–587 (2005)
- Derili, H.A., Sohrabi, S., Arzhang, A.: Two-dimensional wavelets for numerical solution of integral equations. *Math. Sci.* **6**(1), 5 (2012)
- Panjaa, M.M., Mandal, B.N.: Evaluation of singular integrals using Daubechies scale function. *Adv. Comput. Math. Appl.* **3**, 64–75 (2012)
- Lowengrub, M.: Systems of Abel type integral equations in function theoretic methods in differential equations. In: Gilbert, R.P., Weinacht, R.J. (eds.) *Research Notes in Math*, pp. 277–296. Pitman Publishing, London (1976)
- Lowengrub, M., Waltson, J.: System of generalized Abel equation. *SIAM J. Math. Anal.* **10**(4), 794–807 (1979)
- Walton, J.: System of generalized Abel's integral equation with applications to simultaneous dual relations. *SIAM J. Math. Anal.* **10**(4), 808–822 (1979)
- Mandal, N., Chakrabarti, A., Mandal, B.N.: Numerical solution of a system of generalized Abel's integral equation using fractional calculus. *Appl. Math. Lett.* **9**(5), 1–4 (1996)
- Mandal, B.N., Chakrabarti, A.: Applied singular integral equations, pp. 231–239. CRC Press, Cambridge (2016)
- Jafarian, A., Nia, S.A.M., S., Golmankhaneh, A.K., Baleanu, D.: On Bernstein polynomials method to the system of Abel integral equations. In: *Abstract and Applied Analysis* 2014, Hindawi (2014)
- Jafarian, A., Nia, S.A.M., Golmankhaneh, A.K., Baleanu, D.: Numerical solution of linear integral equations system using the Bernstein collocation method. *Adv. Differ. Equ.* **2013**(1), 123 (2013)
- Daubechies, I.: Ten lectures on wavelets. *CBMS-NSF Regional Conference Series in Applied Mathematics*, vol. 61. Society for Industrial and Applied Mathematics (SIAM), Philadelphia, PA (1992). <https://doi.org/10.1137/1.9781611970104>
- Gu, J.S., Jiang, W.S.: The Haar wavelets operational matrix of integration. *Int. J. Syst. Sci.* **27**, 623–628 (1996)
- Giraud, L., Langou, J., Rozloznic, M.: The loss of orthogonality in the Gram-Schmidt orthogonalization process. *Comput. Math. Appl.* **50**(7), 1069–1075 (2005)
- Yousefi, S.A.: B-polynomial multiwavelets approach for the solution of Abel's integral equation. *Int. J. Comput. Math.* **87**(2), 310–316 (2010)
- Pandey, S., Dixit, S., Verma, S.R.: New stable numerical inversion of generalized Abel integral equation. In: Deep, K., Jain, M., Salhi, S. (eds.) *Logistics, Supply Chain and Financial Predictive Analytics. Asset Analytics (Performance and Safety Management)*. Springer, Singapore (2019)
- Singh, V.K., Postnikov, E.B.: Operational matrix approach for solution of integro-differential equations arising in theory of anomalous relaxation processes in vicinity of singular point. *Appl. Math. Model.* **37**(10–11), 6609–6616 (2013)
- Dixit, S., Singh, O.P., Kumar, S.: A stable numerical inversion of generalized Abel's integral equation. *Appl. Numer. Math.* **62**(5), 567–579 (2012)
- Alpert, B.K.: A class of bases in L^2 for the sparse representation of integral operators. *SIAM J. Math. Anal.* **24**(1), 246–262 (1993)
- Nemati, S.: Numerical solution of Volterra-Fredholm integral equations using Legendre collocation method. *J. Comput. Appl. Math.* **278**, 29–36 (2015)

Publisher's Note Springer Nature remains neutral with regard to jurisdictional claims in published maps and institutional affiliations.